Hamlyn Symposium on Medical Robotics 2022

10.31256/HSMR2022.40

Toward Targeted Therapy in the Brain by Leveraging Screw-Tip Soft Magnetically Steerable Needles

Trevor J. Schwehr[1], Adam J. Sperry[1], John D. Rolston[2], Matthew D. Alexander[2,3], Jake J. Abbott[1], and Alan Kuntz[4]

[1]*Department of Mechanical Engineering,* [2]*Department of Neurosurgery,* [3]*Department of Radiology and Imaging Sciences, and* [4]*School of Computing, University of Utah*
alan.kuntz@utah.edu

INTRODUCTION

Steerable needles capable of taking curvilinear trajectories through tissue enable the ability to avoid anatomical obstacles and home in on targets [1]. Steerable needle designs that are pushed into tissue from their base struggle to take tight curvatures without damaging tissue due to the needle cutting laterally through tissue [2]–[4]. We propose a new type of steerable needle that can take much tighter curvatures safely. This needle pulls itself through tissue via a screw tip, with rotation $\boldsymbol{\omega}$ imparted at its base (Fig. 1(a)), either by hand or with a robotic insertion system. The needle is steered by applying a magnetic field $\boldsymbol{b}$ (units T), and thus a magnetic steering torque $\boldsymbol{\tau} = \boldsymbol{m} \times \boldsymbol{b}$ (units N·m), to a magnetic dipole $\boldsymbol{m}$ (units A·m^2) at the needle's tip via, e.g., an external permanent magnet. As the needle's body only needs to transmit rotation to its tip and not an axial insertion force, our design leverages extremely soft tubing for its shaft, which enables the shaft to have low bending stiffness and impart low forces on surrounding tissues. We note that magnetic torque scales with distance as $\|\boldsymbol{\tau}\| \propto d^{-3}$, which is more favorable at clinical scale than force $\|\boldsymbol{f}\| \propto d^{-4}$ [5], which has been proposed as a way to pull soft steerable needles in tissue [6].

Our design enables paths with high curvature, unlocking clinical applications such as targeted therapy in brain tissue. Consider the case of stereotactic ablation in which the hippocampus and the amygdala are ablated via energy application (e.g., laser or radiofrequency) in order to treat epilepsy [7] (Fig. 1(b)). To minimize damage to healthy brain tissue, this procedure is currently performed by inserting a straight instrument into the structures and ablating in a series of cylindrical shapes. Unfortunately, due to the straight nature of the tool, the desire to not ablate brain tissue outside of these structures, and the inability to safely create multiple passes at these brain structures, this results in only partially ablating the intended structures [8].

This work was supported in part by the National Science Foundation under Grant 1830958. T. J. Schwehr and A. J. Sperry contributed equally. T. J. Schwehr is now with the Department of Mechanical Engineering, Johns Hopkins University.

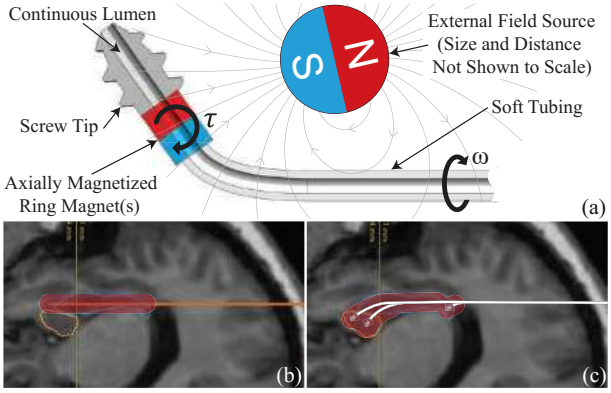

Fig. 1 (a) Cross-section schematic of the needle concept and depiction of the field of an external permanent magnet being used to steer the needle. Our two control variables are $\boldsymbol{\omega}$ and $\boldsymbol{\tau}$. (b) Straight needle insertion and region of ablation with sub-optimal coverage of the hippocampus (blue) and amygdala (orange). (c) Steerable needle insertion and possible region of ablation with three branching paths that more closely follow the shape of the hippocampus and amygdala.

In this work, we demonstrate the ability to leverage our highly curved needle to more closely conform to these brain structures' complex geometries, conceptually opening the door to better ablation patterns (where the ablation probe could be delivered through, or embedded in, the lumen of the steerable needle). To do so, our needle takes a complex path that incorporates multiple branching points wherein our needle is partially retracted and then steered forward along new paths (Fig. 1(c)). We demonstrate such a complex, multi-branch path in brain simulating gelatin, covering a planar representation of the relevant brain structures segmented from the real patient scan of Fig. 1, at correct anatomical scale.

MATERIALS AND METHODS

Our prototype needle (Fig. 2(a)) is constructed from the tip of a No. 2 brass screw (major dia. 2.2 mm, minor dia. 1.4 mm) with a machined lumen of 0.5 mm dia. The screw tip is affixed to four axially magnetized Grade-N50 NdFeB ring magnets—each with 0.5 mm inner dia. (ID), 1 mm outer dia. (OD), 0.5 mm height—acting as one large magnet. They are affixed using cyanoacrylate

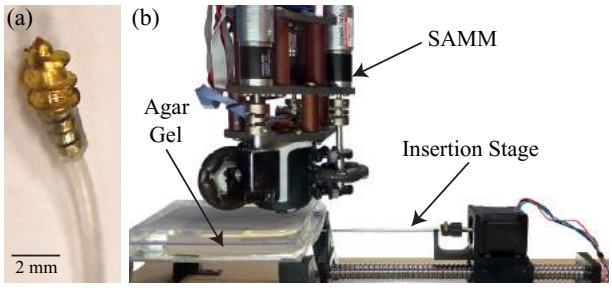

Fig. 2 (a) Image of the tip of the needle prototype. (b) Experimental setup with the SAMM positioned above the tip of the needle in the agar gel. The needle is inserted via a robotic insertion stage.

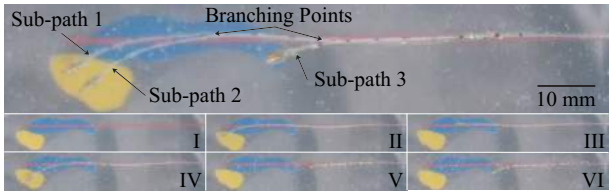

Fig. 3 (Top) Composite image of the branching paths achieved with our needle, with at-scale image of brain structures. (Bottom) Chronological image sequence.

to a Tygon tube with 0.25 mm ID and 0.76 mm OD.
We inserted our needle into a custom 25 mm thick 0.5 wt% agar gel phantom (Fig. 2(b)) that has been previously established to have similar mechanical properties to human brain [9]. A robotic stage inserts the needle by rotating the needle at its base and simultaneously moving forward in a coordinated fashion. We generate the torque at the needle tip to achieve steering by actively actuating the spherical-actuator-magnet manipulator (SAMM) to change the applied magnetic field using its 50.8 mm diameter spherical permanent magnet [10]. In our experiments we repositioned the SAMM periodically during insertion to be directly above the needle tip with steering torque in the desired direction of curvature.
A correctly scaled image of the brain, with the hippocampus and the amygdala regions highlighted, was placed above the agar gel such that it could be seen through the agar by a camera below. Closing the loop visually, a human operator then attempted to steer a three-branched, curved trajectory that ensured that the aggregate path covered the geometry of both brain structures assuming cylindrical ablation around the needle tip trajectory (see Fig. 1(c) for the desired trajectory).

RESULTS

Figure 3 shows a three-stage branching path achieved by our needle. Sub-path 1 is the first insertion of the needle. Sub-paths 2 and 3 were achieved by partially retracting the needle to the respective branching point then reinserting while steering in the new direction of each sub-path. We achieved a 26 mm minimum radius of curvature using an applied field strength of 73 mT.
We performed additional experiments to verify the ability to: steer in 3D, by steering out of the horizontal plane (Fig. 4(a)); and advance through, and steer in, *ex vivo* ovine brain tissue (Fig. 4(b)).

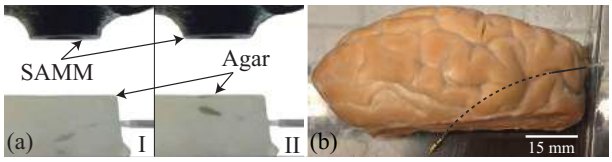

Fig. 4 (a) Demonstration of out-of-plane steering (side view). We steered down (I), partially retracted, then steered up (II). (b) Example of steering through ovine brain (top-down view). We steered the needle open-loop by estimating the needle tip's pose based on expected curvature and translation. In this case, the needle was rotated at its base by hand rather than with the robotic insertion stage. Due to the open-loop nature of this experiment, this curvature should not be assumed maximal.

DISCUSSION

These results demonstrate the potential of this needle design to precisely navigate with high curvature to a particular region of interest in the brain for targeted therapies such as energy-based ablation. They further demonstrate the potential to take branching paths when necessary, potentially enabling complete coverage of a region while minimizing travel through healthy tissue.
We note that, given that the OD of the commercial ring magnets we employ in this work is smaller than the minor diameter of the screw tip in our prototype, we could increase the steering torque by 117% via custom magnets, or we could decrease the size of our screw tip by 27% via a custom screw (potentially with a different material and/or thread height as well).
Magnetic steering requires knowledge of the five-degree-of-freedom pose of the needle's tip. In our closed-loop experiments this was possible due to the transparency of the phantom, but limited our experiments to be in a plane. To further evaluate the performance of this needle in opaque tissues (such as the brain) with 3D regions of interest, closed-loop control and localization without line-of-sight is required. Such localization can be achieved through medical-imaging (e.g., CT, fluoroscopy) or potentially through magnetic localization.

REFERENCES

[1] R. J. Webster III *et al.*, "Nonholonomic modeling of needle steering," *Int. J. Robot. Res.*, vol. 25, no. 5-6, pp. 509–525, 2006.
[2] K. B. Reed *et al.*, "Robot-assisted needle steering," *IEEE Robot. Autom. Mag.*, vol. 18, no. 4, pp. 35–46, 2011.
[3] M. Rox *et al.*, "Decoupling steerability from diameter: Helical dovetail laser patterning for steerable needles," *IEEE Access*, vol. 8, pp. 181 411–181 419, 2020.
[4] A. Hong *et al.*, "Magnetic control of a flexible needle in neurosurgery," *IEEE Trans. Biomed. Eng.*, vol. 68, no. 2, pp. 616–627, Feb. 2021.
[5] J. J. Abbott *et al.*, "Magnetic methods in robotics," *Annu. Rev. Control Robot. Auton. Syst.*, vol. 3, pp. 57–90, 2020.
[6] M. Ilami *et al.*, "Magnetic needle steering in soft phantom tissue," *Sci. Rep.*, vol. 10, p. 2500, 2020.
[7] M. Cossu *et al.*, "RF-ablation in periventricular heterotopia-related epilepsy," *Epilepsy Res.*, vol. 142, pp. 121–125, 2018.
[8] S. S. Grewal *et al.*, "Laser ablation for mesial temporal epilepsy: a multi-site, single institutional series," *J. Neurosurg.*, vol. 130, pp. 2055–2062, 2018.
[9] D. C. Stewart *et al.*, "Mechanical characterization of human brain tumors from patients and comparison to potential surgical phantoms," *PLOS ONE*, vol. 12, no. 6, p. e0177561, Jun. 2017.
[10] S. E. Wright *et al.*, "The spherical-actuator-magnet manipulator: a permanent-magnet robotic end-effector," *IEEE Trans. Robot.*, vol. 33, no. 5, pp. 1013–1024, 2017.